Chronostratigraphic interpretation of airborne electromagnetics in the Halls Creek–Birrindudu–Tanami region

Sebastian Wong[1,2] *and Malcolm Nicoll*[1]

Introduction

As part of the *Resourcing Australia's Prosperity* initiative, led by Geoscience Australia (GA), several deep dive regions have been established to enhance understanding of resource prospectivity in selected onshore locations. One such region is the Birrindudu Deep Dive (BDD), which straddles the Northern Territory and Western Australia border. As part of this deep dive, geological interpretation of selected lines from the AusAEM 02 WA/NT 2019–20 Airborne Electromagnetic (AEM) Survey (Ley-Cooper 2020), along with supporting datasets and information, is underway (**Figure 1a**,**b**).

The interpreted AEM dataset comprises approximately 11 250 km of conductivity sections with a 20 km nominal line spacing across an area over 200 000 km^2 – an area almost the size of the state of Victoria. This interpretation contributes to the national-scale chronostratigraphic interpretation of AEM, which currently covers over

[1] Geoscience Australia, Cnr Jerrabomberra Ave and Hindmarsh Drive, Symonston ACT 2609, Australia
[2] Email: Sebastian.Wong@ga.gov.au

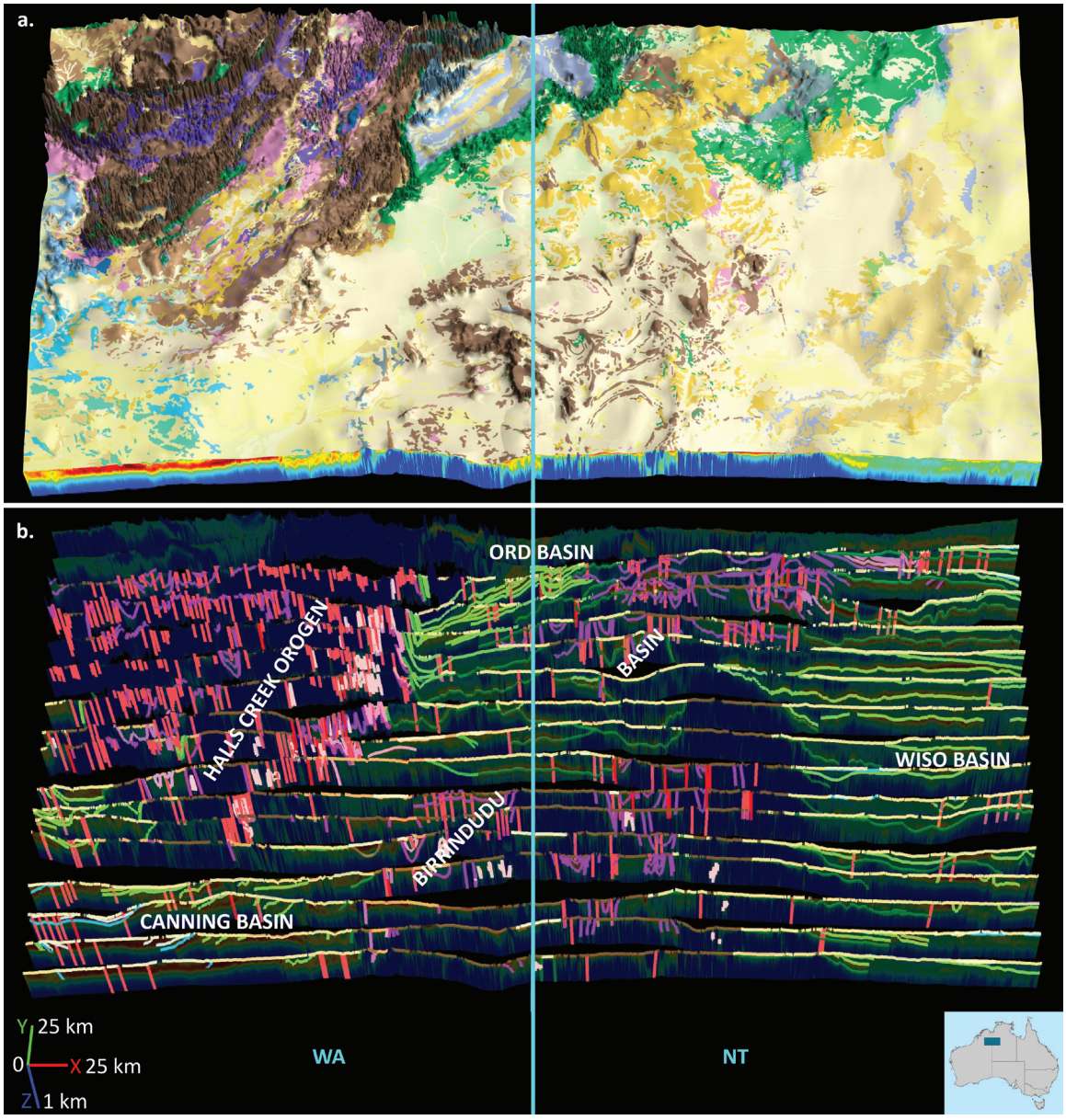

Figure 1. Birrindudu Deep Dive (BDD) chronostratigraphic AEM interpretation study area. (**a**) *Surface Geology of Australia, 1:1 000 000 scale, 2012 edition* (Raymond 2012) draped on a digital elevation model showing outcropping Proterozoic rocks (browns, purples and pinks), overlain by volcanics (dark green), Palaeozoic basins (blues), and widespread Cenozoic cover (yellows). Please see Raymond (2012) for the complete surface geology legend. (**b**) The status of chronostratigraphic AEM interpretation showing the location of key geological features discussed herein. Interpretation superimposed on transparent conductivity sections of Ley-Cooper (2020). Please see Wong *et al* (2022) for the AEM interpretation legend.

115 000 km of AEM flight lines across approximately 27% of the Australian continent. These interpretations provide multidisciplinary datasets that can be used for a wide range of geological studies. For example, they are currently used in cover thickness modelling (eg Bonnardot *et al* 2025, Vizy *et al* 2025), which is, in turn, used in prospectivity mapping (eg Ford *et al* 2026a,b) and economic viability modelling (eg Haynes *et al* 2020).

The AEM interpretation in the BDD region continues this multidisciplinary approach by providing insight into the depth and subsurface distribution of stratigraphic units and other geological features. Mapping the subsurface geology is intended to establish constraints in areas where depth-estimate data are limited and subsurface stratigraphic unit boundaries are poorly defined. This helps constrain the resource prospectivity, stratigraphic relationships, basin configurations and general geological evolution of the region. Features valuable to a range of disciplines are mapped and commented on, such as discrete electrical conductors in areas of mineralisation; palaeovalleys as potential sources of groundwater; and faulting or neotectonic features. This multidisciplinary approach means that academia, government and industry can use these interpretations for a wide range of purposes, including resource exploration and management, environmental monitoring, hazard mapping, tectonic research, land-use planning and decision-making.

Methods

The AEM data were inverted using the Geoscience Australia deterministic layered-earth inversion (GA-LEI; Brodie 2016, Ley-Cooper 2020) and the High Quality Geophysical Analysis (HiQGA) probabilistic inversion code (Ray *et al* 2023a,b, Ray *et al* 2024). Both methods generated conductivity sections that were directly used in the interpretation.

Several additional inputs were generated to facilitate digitisation and integration of data, which ensured that comprehensive, high-quality interpretations were produced. A process was developed to georeference the deterministic and 10th, 50th and 90th percentiles of the probabilistic inversions for simultaneous interpretation in geographic information systems (GIS). Another interpretation aid was the extraction of map data along AEM flight lines and plotting of this data adjacent to the conductivity sections in GIS. This ensures that data from the *Surface Geology of Australia, 1:1 000 000 scale, 2012 edition* (Raymond 2012), each layer in the *Layered Geology of Australia, 1:1 000 000 scale, 2024 edition* (Sanchez *et al* 2024), and the geoscientific thematic map of Australia's arid and semi-arid zone palaeovalley systems in WA, SA and the NT (WASANT; Bell *et al* 2012) were considered during the interpretation. Further aids such as maps of flight lines taken, surface elevation, depth horizons, and bounding boxes were also produced to ensure spatial accuracy and assist interpretation. For more detail on these aids, refer to Nicoll *et al* (2025, 2026).

The conductivity sections were interpreted using the multilayered chronostratigraphic AEM interpretation workflow (Wong *et al* 2022) which facilitates the integration of AEM conductivity sections with supporting data (such as surface and solid geology maps, the geophysics of potential fields, boreholes, mineral occurrences, palaeovalleys, etc) in both 2D and 3D spaces. Important information in these supporting datasets was extracted and attributed to interpretation lines and points using this workflow.

The main aim of the interpretation is delineating the contacts between major chronostratigraphic boundaries, such as the contacts between different geological eras. If a discernible contact lies within a geological era, these are also captured. Other geological features are interpreted, including faults, groundwater-related information and discrete electrical conductors. When interpreting discrete electrical conductors, various factors, including local geological features, infrastructure and inversion artefacts are considered. After careful elimination, conductors are mapped, and detailed comments about their possible origins and, in some cases, possible links to mineralisation, are captured.

Each chronostratigraphic interpretation line or point is attributed with the geological era, names, numbers and confidences of the stratigraphic units above and below the interpretation – consistent with the Australian Stratigraphic Units Database (ASUD; Raymond and Brown 1949; https://asud.ga.gov.au/) – as well as confidences for the interpretation placement location, the basis of interpretation (what datasets were used to inform the interpretation), and so on. 'Comments' and 'New Observation' fields allow the interpreter to attribute additional information and provide background on the thought processes involved in deriving the interpretation. This rich interpretation-specific information allows users to thoroughly interrogate the dataset.

Interpretations made using this procedure are processed using code developed at GA specifically designed for validating and converting the interpretations to various formats (Wong *et al* 2022, Nicoll *et al* 2025). Validation of input files ensures that interpreted conductivity section and flight line information match and are correctly located. Postinterpretation validation incorporates checking stratigraphic information against ASUD for typographical errors, mismatched names and numbers, and unit currency. This process also validates interpretation geometries, and automatically adjusts certain geometric errors.

Following validation, the workflow converts the interpretation to various formats. These formats include 3D polylines, for visualisation on the Geoscience Australia Portal (https://portal.ga.gov.au/3d) and other 3D software. Point data in XYZ format are also exported for direct upload to the GA Estimates of Geological and Geophysical Surfaces (EGGS) database (Mathews *et al* 2020; https://portal.ga.gov.au/restore/7734b152-d8a7-4e3c-8efc-1dd3ba37db5f) and other software packages. Past interpretations can be viewed and downloaded in point form from EGGS, alongside curated depth estimates from other disciplines (eg boreholes, depth to magnetics). They can also be downloaded as standalone packages from the GA electronic catalogue (eCat). (https://ecat.ga.gov.au/geonetwork/srv/eng/catalog.search#/home)

Results

Interpretation of the AusAEM, plus supporting datasets, in the BDD region has provided an unprecedented view of the near-surface geology. The following are examples of some key observations and results from this study.

Depth estimates

This interpretation has currently captured ~4200 interpretation lines (**Figure 1b**), including ~44 000 depth estimates points, which provide a novel dataset that can be used by a range of stakeholders.

Due to the regional coverage of the interpreted survey, this interpretation provides both additional insight into well-mapped areas and new information to constrain poorly understood geology. This broad-stroke method enhances knowledge of the chronostratigraphic configuration and can contribute to improving surface and solid geology datasets. The resultant datasets can also be used to improve cover and hydrostratigraphic models and for quality control of other depth-estimate datasets, such as boreholes and depth to magnetic anomalies.

The depth estimates show sediment thicknesses over potentially prospective basement rocks, which can be queried to interrogate the stratigraphic unit information to explore the depth to, and spatial distribution of, subsurface stratigraphic units of interest. Ultimately, this dataset can be used by researchers and explorers to determine if a specific stratigraphic unit occurs in their area of interest; and if so, its depth and spatial distribution.

Delineating basin boundaries

The basin to basement boundary contacts have been mapped over large areas where there is a conductivity contrast or marker horizon with a specific conductivity response. In the central and east parts of the region, the base of Palaeozoic basins (eg the Ord and Wiso basins) can be mapped at depth for great distances from the rare instances of the outcropping contact. Throughout these areas, boreholes are sparsely distributed and few intersect the base of the basins and underlying basement. However, the conductivity contrast between the resistive basements and the moderately conductive basins helps delineate this contact. In some areas, the base of the Antrim Plateau Volcanics, which is typically the basal unit in these basins, is associated with a distinct, highly conductive horizon. This conductive horizon could be the result of weathering and/or lithological and hydrological factors.

Correlation between the conductive horizon occurring at Palaeozoic basin to Proterozoic basement contacts suggests that this horizon is a marker for the base of the Palaeozoic basins. This data presented an opportunity to map the base of the basins over large areas. This is particularly advantageous as there is limited knowledge of the basin thicknesses over large parts of the region due to the paucity of depth estimates providing constraints on the depth of the basins; coupled with the widespread Antrim Plateau Volcanics impeding interpretation of the underlying rocks in the magnetic grids. This new interpretation provides an insight into the geometry of these contacts, the thicknesses of the basins, and the relationship between the basement, the Antrim Plateau Volcanics, and the basin sediments.

Likewise, in the southwest of the study region, the Canning Basin has been mapped. Here, the steeper contact between the underlying basement and the thick basin sediments, as well as the highly conductive nature of some of the overlying sediments resulted in a reduced ability to map the base of the Canning Basin across large areas. Despite this, the internal stratigraphy could be well mapped because of the conductivity contrast between certain stratigraphic units. The contact between Mesozoic and Palaeozoic stratigraphy could also be mapped confidently in some areas.

Where the basin margins are obscured by widespread Cenozoic cover, the location of the basin boundaries could be refined using the AEM. In some cases, basin boundaries in certain datasets, such as the *Australian Geological Provinces, 2018.01 edition* (Raymond *et al* 2018) and *Layered Geology of Australia 1:1 000 000 scale, 2024 edition* (Sanchez *et al* 2024) were drawn based on interpolation between rare, scattered outcrops, interpretation of geophysical data and/or borehole intersections. The regional AusAEM dataset presents an opportunity to revise some of these basin boundaries based on the ability of this geophysical method to image through the widespread cover.

Mineral occurrences

One of the benefits AEM offers mineral explorers is its ability to image features that could be related to mineralisation, especially within the typical search space of the top 500 m. This interpretation maps discrete electrical conductors with a dedicated feature type, which can be used by mineral explorers to immediately show their locations, and can be interrogated for additional information about possible links to specific mineral occurrences or commodities.

The study region hosts a range of mineral occurrences including gold, silver, lead, copper, tin, tantalum, niobium and graphite. Where discrete electrical conductors were observed, mineral occurrence datasets were integrated with the AEM to understand potential sources of the conductors. Commonly, precious and base metal occurrences and graphite deposits were found to be associated with these discrete electrical conductors. These observations are consistent with studies investigating the conductivity response of earth materials, showing some mineral types, such as massive sulphides and graphite, to have high electrical conductivity (eg Palacky 1987).

Following a comprehensive approach to discount inversion artefacts, anthropogenic and non-geological sources of the discrete electrical conductors, the remaining conductors were delineated. These mapped conductors are typically accompanied by detailed comments and other information to provide users with the supporting information and methodology used to determine their presence.

This dataset provides mineral explorers with information to gauge the depth to potential mineralisation, and the subsurface geometries and spatial distributions of mineral deposits and host rocks. One such example

is in the Halls Creek Orogen and Lamboo Province area, where the subsurface is generally dominated by resistive Palaeoproterozoic rocks, such as metamorphic and igneous rocks of the Halls Creek Group and Sally Downs Supersuite. Here, precious and base metals, and graphite occurrences exist (Sexton 2011). The conductive nature of the mineralisation provides a sharp contrast to the resistive country rocks, making the area a valuable study site for investigating the relationship between discrete electrical conductors, mineral occurrences and structural trends.

For example, known precious and base metal occurrences in the Olympio Formation of the Halls Creek Group coincide with discrete electrical conductors in the AEM. These mineral occurrences have previously been mapped at the surface; however, observations of discrete electrical conductors directly below them provide the opportunity to understand the subsurface distribution of the mineralisation.

Likewise, in this area, known graphite occurrences coincide with AEM flight lines and have been intersected by boreholes. Here, the resistive host rocks provide a stark contrast to the discrete highly conductive anomalies dispersed throughout the area (**Figures 2** and **3**). Correlations between these discrete electrical conductors with the mapped graphite occurrences and graphite-intersecting

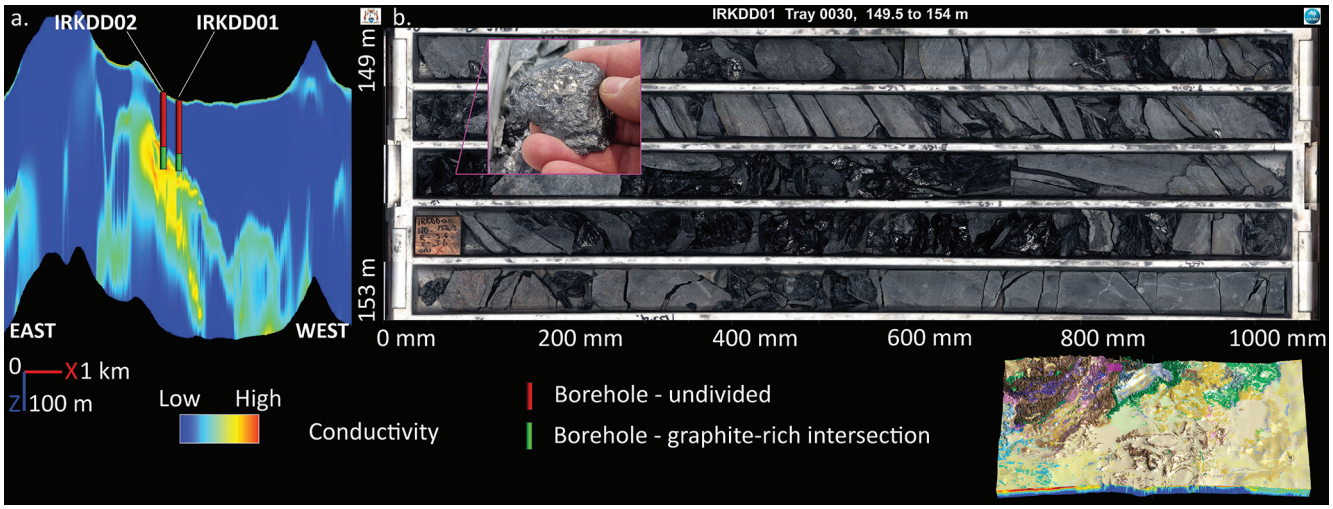

Figure 2. Example of discrete electrical conductors correlated with borehole graphite intersections. (**a**) Part of flight line 5002002 from the AusAEM 02 Survey (Ley-Cooper 2020) with nearby boreholes IRKDD01 and IRKDD02 projected to the line. (**b**) Representative borehole tray photograph of graphite-rich rock from IRKDD01 (AuScope 2026); (inset) Detail of graphite-rich hand specimen from ~151 m downhole of IRKDD01.

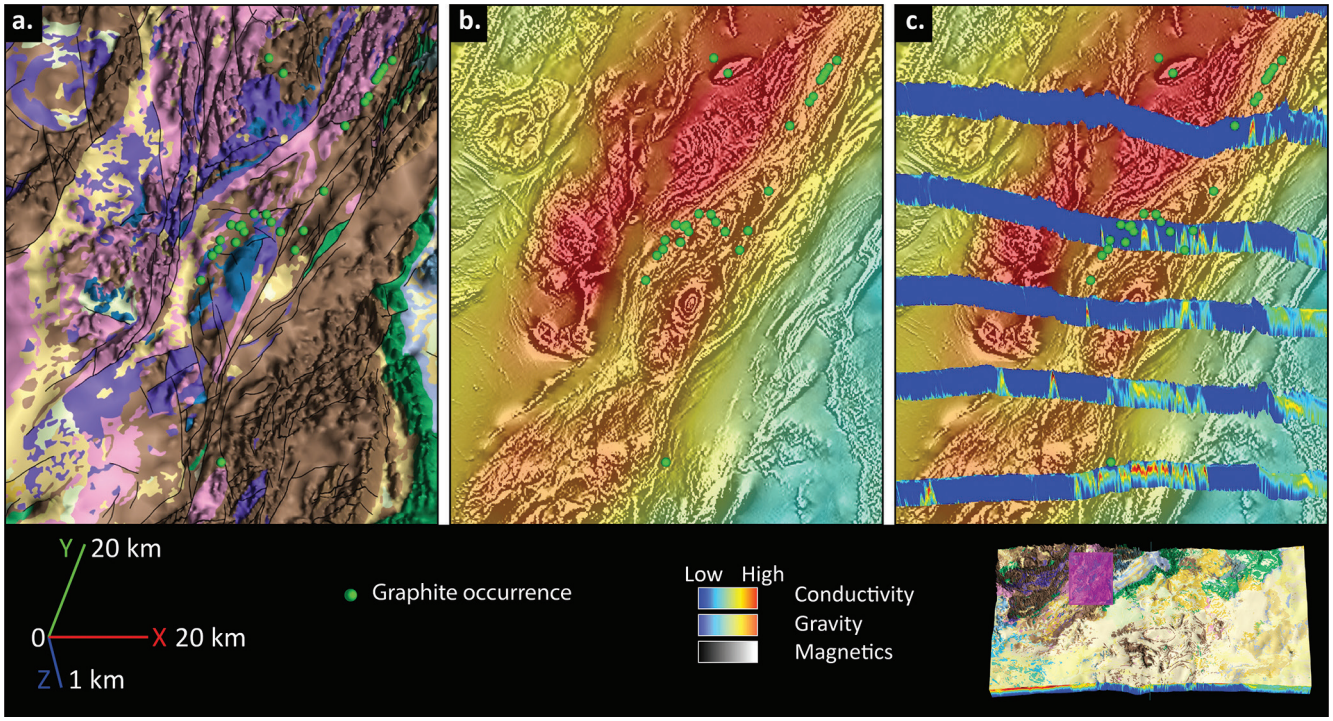

Figure 3. Relationship between discrete electrical conductors observed in the AEM, graphite occurrences, geological units, structural features and potential fields datasets. (**a**) Graphite occurrences (Sexton 2011) occurring on stratigraphic contacts and along faults. Please see Raymond (2012) for the complete surface geology legend. (**b**) Graphite occurrences and their correlation to structural trends seen in the magnetics (Poudjom Djomani and Minty 2019) and gravity (Geophysical Acquisition & Processing Section 2020) potential fields datasets. (**c**) Discrete electrical conductors observable in the AusAEM dataset (Ley-Cooper 2020). Note discrete electrical conductors in areas of no documented graphite occurrences, which occur along structural trends from documented occurrences. Please note also that there is a slight offset between the graphite occurrences and the other datasets due to the oblique 3D view.

boreholes provide strong evidence that the conductors are related to graphite mineralisation (**Figure 2**).

Furthermore, consideration of these discrete electrical conductors and graphite occurrences alongside geological, faults and potential fields datasets, suggest that they are structurally and/or stratigraphically controlled, as they typically occur in areas of faulting and along stratigraphic contacts (**Figure 3a**). As the discrete electrical conductors associated with graphite mineralisation typically occur along fault planes and stratigraphic contacts observable in the geology maps, magnetic grids, or along steep gravity gradients, the geological and potential fields datasets can be used to extrapolate the distribution of mineralisation.

In many cases, geological and potential fields datasets have helped to extrapolate potential precious and base metals, and graphite mineralisation along structural trends away from the flight lines. Interestingly, similar discrete electrical conductors have been observed along these structural trends on adjacent flight lines, where no mineral occurrences have previously been mapped. This suggests that AEM can be used to highlight potential areas of undocumented mineralisation.

This interpretation could help explorers to both broaden their search areas while also constraining their exploration targets. The mapping of discrete electrical conductors, as well as the detailed commentary accompanying them, means that explorers can filter for these features in the interpretation dataset, plot them spatially and interrogate the additional information regarding the correlation of various datasets used to support the interpretation.

Structures

Integration of the AEM models with surface geology maps and magnetic grids in 3D space facilitated a joint interpretation of structural features. Within structurally deformed domains, typically in the Palaeoproterozoic rocks, structural features, such as faults and folds, have previously been mapped in surface geology maps. Where the AEM flight lines intersect these structural features, the structural trends could be interpolated along the AEM conductivity sections. Correlating the structural measurements on maps (such as strikes, dips, antiforms, synforms, and fold axial trace trends and plunges) with features observed in the AEM allowed for the mapping of these structural features in 3D.

Where there were stratigraphic units that had distinct electrically conductive responses, these units could be used to map the subsurface geometries of the structural features. In the cases of folded stratigraphy, the AEM could be used to link repeated units at the surface by delineating the fold hinges at depth (eg indicated by the purple linework in **Figure 1b**). The magnetic grids were used to support these interpretations, as they provide insight into the structural trends beneath the widespread Cenozoic cover. Correlation between the AEM, surface geology maps and magnetic grids increased confidence that the structural features observed in the AEM are geological and helped constrain these interpretations. Several large-scale folds in the Birrindudu and Tanami groups could be mapped with confidence using this approach.

Palaeovalley mapping

This interpretation has highlighted areas where further investigations are warranted and where inconsistencies between certain datasets exist. For example, the AEM conductivity sections were integrated with the WASANT palaeovalley map (Bell *et al* 2012) in 3D, which helped to analyse the intersection of the previously mapped palaeovalleys and the electromagnetic responses. In areas such as this, palaeovalleys are usually observed as conductive features with channel-like geometries overlying, or incised into, resistive basement rocks. Using the AEM allows interpreters to not only consider the location of the mapped palaeovalleys, but also their 3D geometries and relationships to the underlying rocks. This method not only facilitates revising the spatial distributions of mapped palaeovalleys but also presents the opportunity to identify those which have previously not been mapped.

Interestingly, the AEM showed that the spatial distributions of some palaeovalleys of Bell *et al* (2012) have likely been overestimated across the region (**Figure 4**). In certain areas where the WASANT dataset has palaeovalley polygons, the AEM conductivity sections suggest only a thin (~10 m) veneer of conductive unconsolidated Cenozoic sediments cover resistive basement rocks. Furthermore, in many of these areas, the thin near-surface conductive horizon has not only been interpreted as Cenozoic sediments but also includes a conductive weathering profile in the uppermost portion of the basement rocks. If this interpretation is correct, it further reduces the interpreted thickness of the overlying Cenozoic sediments. These observations suggest that there are thin to no palaeovalleys occurring in such areas, despite being mapped in the WASANT dataset. Understandably, as the regional AusAEM was not available at the time of mapping the palaeovalleys in the WASANT dataset. However, what this does prove, is that regional AEM datasets are excellent tools to be considered in future regional palaeovalley mapping exercises.

By comparison, in the central Northern Territory, large palaeovalleys with thicknesses over 200 m and continuous lengths of over 400 km have been observed as conductive palaeovalley fill over resistive basement rocks (Wong *et al* 2023). Observations such as those in this study and in the central Northern Territory demonstrate the value of AEM to not only revise the spatial distributions, depths and presence of palaeovalleys, but also map palaeovalleys in 3D over large regions.

Additionally, the electromagnetic response provides insight into the composition of the underlying rocks, which can help groundwater explorers understand if the substrate to the palaeovalley is acting as an aquitard (eg in the case of highly resistive nonporous crystalline basement rocks), or as a fluid flow conduit or aquifer (eg in the case of moderately conductive porous sandstone). The robustness of such interpretations is greatly improved when the AEM is integrated with other geological datasets, such as maps and boreholes, to help constrain the hydrolithological characteristics of the covered basement.

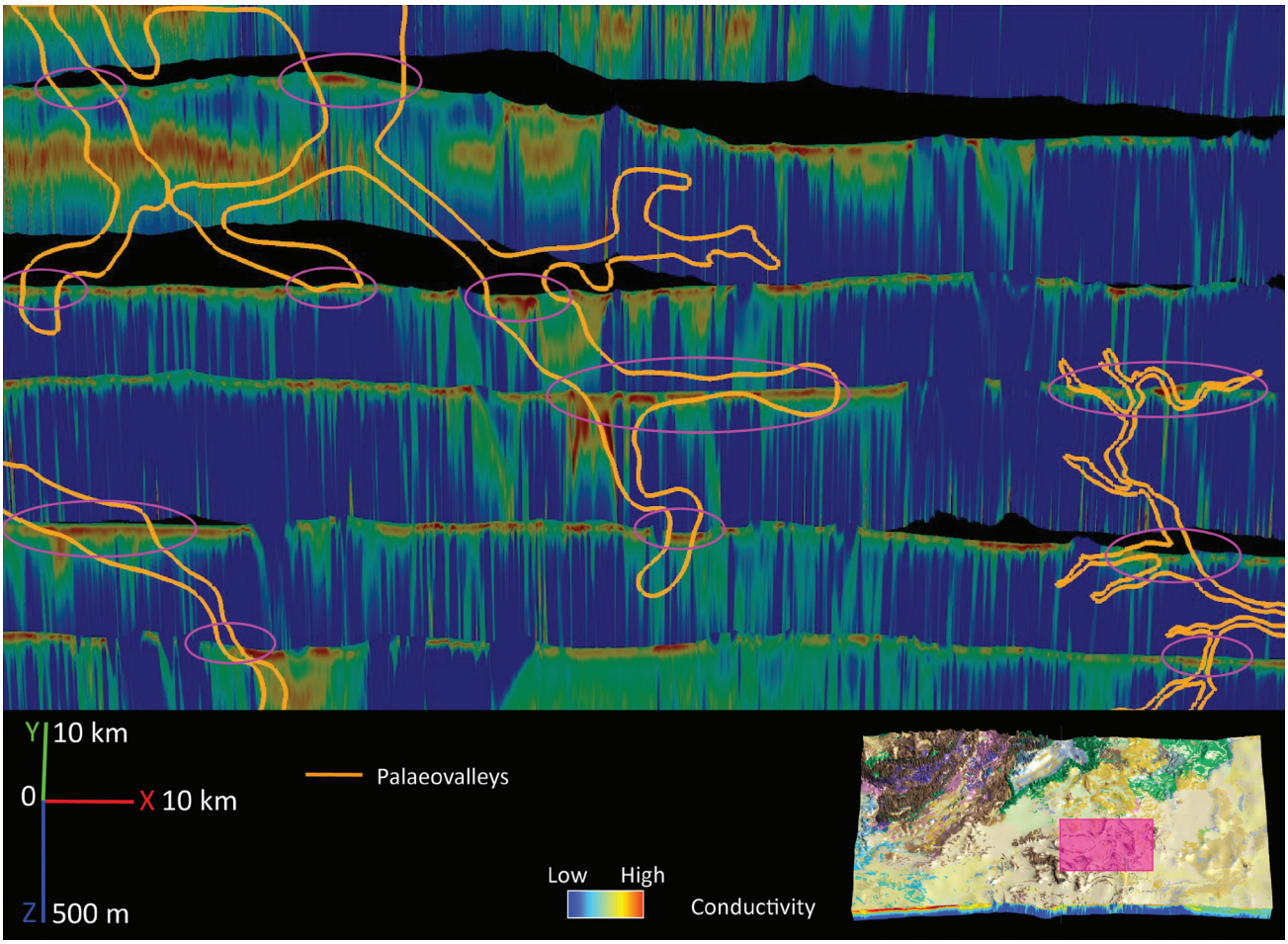

Figure 4. Intersections (pink ellipses) between AusAEM conductivity sections (Ley-Cooper 2020) and the WASANT palaeovalley polygons (Bell *et al* 2012). Limited channel-like geometries are observed in this area. It is interpreted that only a thin veneer of Cenozoic sediments overlies a conductive weathering horizon in the uppermost portion of the resistive Proterozoic basement in this area.

Discussion and conclusions

The AEM interpretation in the BDD region adds to the national-scale chronostratigraphic interpretation of AEM and provides an information-rich dataset that delineates the 3D geometries and describes specific information about the stratigraphy and other features across the region. The interpretation has enhanced understanding of the basin configuration in the region, especially for the thicknesses and basal geometries of Palaeozoic basins. Furthermore, it provides information on the stratigraphic units below these basins and under the widespread Cenozoic cover, which can be used by explorers and researchers interested in the underlying geology.

This dataset highlights areas where previously undocumented mineral occurrences could exist, based on the relationship between discrete electrical conductors, known mineral occurrences, and structural and stratigraphic features. An abundance of chronostratigraphic constraints means the interpretation can also be used to update existing surface and solid geology maps, palaeovalley maps and cover models.

Ultimately, the BDD AEM interpretation and other consistently formatted chronostratigraphic AEM interpretations (produced at GA) are multidisciplinary and are useful for a wide range of users – from mineral explorers and geological mappers to groundwater managers and hazard mappers. It is intended that, upon completion and quality control of this dataset, it will be uploaded to the EGGS database for display and download. This dataset is also being prepared for release as a 3D polyline dataset on the GA Portal, and as a standalone data package in a range of formats on the GA eCat.

Acknowledgements

The authors acknowledge Alan Yusen Ley-Cooper and Anandaroop Ray from the GA Geophysical Acquisition and Processing Section for providing the AEM data and inversions. Emmanuelle Grosjean, Chris Southby and Paul Henson from the GA Onshore Energy Systems Section are acknowledged for their valuable discussions about graphite occurrences in the area and general support of this work. Jackie Hope from the GA Integrated Geological Mapping Section is thanked for discussions on local boreholes. This study was funded by the *Resourcing Australia's Prosperity* initiative.

References

AuScope 2026. *AuScope Discovery Portal, National Virtual Core Library V-2.0.* <https://portal.auscope.org.au/?state=56a89cd5-2f54-4256-be8d-0f6fba9fa98d>. [Accessed 24 February 2026].

Bell JG, Kilgour PL, English PM, Woodgate MF and Lewis SJ, 2012. *WASANT Palaeovalley Map – Distribution of Palaeovalleys in Arid and Semi-arid WA-SA-NT.* Geoscience Australia, Canberra, dataset. https://pid.geoscience.gov.au/dataset/ga/73980

Bonnardot MA, Grose L, Wilford J, Du Z, Hope J, Wong SCT, Vizy J and Rollet N, 2025. *EFTF cover thickness model in the Darling–Curnamona–Delamerian (DCD) region.* Geoscience Australia, Canberra, dataset. doi:10.26186/149732

Brodie RC, 2016. *GA-AEM source code repository.* https://github.com/GeoscienceAustralia/ga-aem

Ford A, Walsh J, Doublier M, Burnham A, Cloutier J, Fraser G, Magee C and Czarnota K, 2026a. *Unconformity-related rare earth element mineral potential of Australia.* Geoscience Australia, Canberra, dataset. https://pid.geoscience.gov.au/dataset/ga/150680

Ford A, Walsh J, Doublier M, Burnham A, Cloutier J, Fraser G, Magee C and Czarnota K, 2026b. *Unconformity-related rare earth element mineral potential maps.* Geoscience Australia, Canberra, dataset. https://pid.geoscience.gov.au/dataset/ga/150681

Geophysical Acquisition and Processing Section, 2020. *National Gravity Compilation 2019 DGIR grid.* Geoscience Australia, Canberra, dataset. https://pid.geoscience.gov.au/dataset/ga/144778

Haynes MW, Walsh SDC, Czarnota K, Northey SA and Yellishetty M, 2020. *Economic Fairways Assessments across Northern Australia.* Geoscience Australia, Canberra. doi:10.11636/133681

Ley-Cooper AY, 2020. AusAEM 02 *WA/NT 2019–20 Airborne Electromagnetic Survey.* Geoscience Australia, Canberra, dataset. https://pid.geoscience.gov.au/dataset/ga/140156

Mathews EJ, Czarnota K, Meixner AJ, Bonnardot MA, Curtis C, Wilford J, Nicoll MG, Wong SCT, Thorose M and Ley-Cooper Y, 2020. *Putting all your EGGS in one basket: the Estimates of Geological and Geophysical Surfaces database.* Geoscience Australia, Canberra, dataset. doi:10.11636/132526

Nicoll M, Wong SCT, Aleksovski T, Ilovski M, Hassan T, Bilic A and Roberts M, 2025. *AEMInterpConvert – Geoscience Australia's Online Airborne Electromagnetic Interpretation Conversion Tool.* Geoscience Australia, Canberra, dataset. https://pid.geoscience.gov.au/dataset/ga/150529

Nicoll MG, Wong SCT, Ley-Cooper AY, Deo RN, Dennis J, Sedgmen A and Ray A, 2026. AusAEM, *Northeast Queensland, Australia, 2024 Airborne Electromagnetic Survey, Conductivity section images, geometry files and interpretation aids for use in the AEMInterpConvert workflow.* Geoscience Australia, Canberra, dataset. https://pid.geoscience.gov.au/dataset/ga/150859

Palacky GV, 1987. Resistivity characteristics of geologic targets: in Nabighian MN and Corbett JD (editors) *'Electromagnetic methods in applied geophysics, Volume 1, Theory'*. Society of Exploration Geophysicists, p 53–129. doi:10.1190/1.9781560802631.ch3

Poudjom Djomani Y and Minty BRS, 2019. *Total Magnetic Intensity Grid of Australia 2019 – First Vertical Derivative (1VD).* Geoscience Australia, Canberra, dataset. doi:10.26186/5dd48b1368ece

Ray A, Douglas A, VanDerWielen S, Ley-Cooper Y, Brodie R, Symington N, Nicoll M, Wong SCT, Sun Y and Czarnota K, 2024. *Probabilistic airborne electromagnetic inversion of 20 km AusAEM data, Phase 1.* Geoscience Australia, Canberra, dataset. doi:10.26186/149375

Ray A, Ley-Cooper Y, Brodie RC, Taylor R, Symington N and Moghaddam NF, 2023a. An information theoretic Bayesian uncertainty analysis of AEM systems over Menindee Lake, Australia. *Geophysical Journal International* 235(2). doi:10.1093/gji/ggad337

Ray A, Taylor R, Brodie RC, Ley-Cooper Y, Symington N and Moghaddam NF 2023b. HiQGA: *Open source deterministic and probabilistic AEM inversion.* doi:110.5281/zenodo.10060343, https://github.com/GeoscienceAustralia/HiQGA.jl/releases/tag/v0.4.12

Raymond OL, 2012. *Surface geology of Australia, 1:1 000 000 scale, 2012 edition.* Geoscience Australia, Canberra, dataset. doi:10.26186/74855

Raymond OL and Brown CE, 1949. *Australian Stratigraphic Units Database (ASUD).* Geoscience Australia, Canberra, dataset. https://pid.geoscience.gov.au/dataset/ga/21884

Raymond OL, Totterdell JM, Woods MA and Stewart AJ, 2018. *Australian geological provinces 2018.01 edition.* Geoscience Australia, Canberra, dataset. doi:10.26186/116823

Sexton M, 2011. *Australian Mineral Occurrences Collection.* Geoscience Australia, Canberra, dataset. https://pid.geoscience.gov.au/dataset/ga/73131

Vizy J, Rollet N and Nicoll M, 2025. Preliminary 3D *Chronostratigraphic model of Australia – Data package of 3D modelling chronostratigraphic surfaces and isochores, Version 1.0.* Geoscience Australia, Canberra, dataset. https://pid.geoscience.gov.au/dataset/ga/149923

Wong SCT, Nicoll M, Brodie R, Hope J, Bonnardot M, Roach I and Ley-Cooper Y, 2022. Multilayered chronostratigraphic airborne electromagnetic interpretation workflow. *Geoscience Australia Record* 2022/37. doi:10.11636/Record.2022.037

Wong SCT, Roach IC, Connors KA, Vilhena JFM, Pitt L, Nicoll MG, Hope JA, Bonnardot M-A, Brodie RC, and Ley-Cooper AY, 2023. Australian continental-scale multilayered chronostratigraphic interpretation of airborne electromagnetics: in *'8th International Airborne Electromagnetics Workshop, Fitzroy Island, 2023'. Australian Society of Exploration Geophysicists Extended Abstracts,* 2023 (2). doi:10.5281/zenodo.10067898